2016 14th International Conference on Control, Automation, Robotics & Vision
Phuket, Thailand, 13-15th November 2016 (ICARCV 2016)

Spatial Projection of Thermal Data for Visual Inspection

Dorit Borrmann*, Florian Leutert†, Klaus Schilling *† and Andreas Nüchter*†
*Informatics VII – Robotics and Telematics,
Julius Maximilian University of Würzburg, Germany
†Center for Telematics, Würzburg, Germany
Email: borrmann@informatik.uni-wuerzburg.de

***Abstract*—Since the advent of thermal imaging, devices with a high optical resolution that use detector arrays to capture the emitted radiance in the thermal infrared range of an entire scene simultaneously have developed as a standard in monitoring energy related aspects. They have had a huge impact on the building industry and in manifacturing, where they are commonly used to monitor proecces that require stable temperature conditions. As beneficial as contactless measurements are, the subsequent localization of points of interest in the environment is often difficult. To overcome this problem we propose a portable system that combines thermal imaging with Augmented Reality (AR). The idea of the approach is to project the gathered temperature information back into the scene to facilitate visual inspection.**

I. Introduction

Thermal imaging refers to the contactless measurement of temperatures by measuring the infrared radiation emitted by any object due to heat. It is the de-facto standard in monitoring energy related issues. Detecting thermal bridges of building walls and analyzing the energy loss - for example through pillars interrupting the thermal insulation or air leaks at windows and doors - is essential to increase the energy efficiency of existing buildings. For quality management it is common to perform thermography before, during and after the construction phase for new buildings or the energetic restauration of exisiting buildings. Other applications aim at documenting and examining the run of heating pipes, detecting blocked pipes and construction units in a building to eliminate flaws, to make room for improvements and, in some cases, to ensure safety (cf. [1]). These applications are not limited to building analysis [2], [3]. In the automotive industry thermal cameras are used in various steps during the manufacturing process, such as the thermoforing of exterior parts and the laminating of interiors. Furthermore, thermal cameras are used for inspection to localize defects at brakes, heating or air conditioning systems. Maintenance of electric systems and air conditioning technology is another application area.

Thermal cameras have two major advantages over other temperature measurement methods. First, contactless measurements allow for precise measurements without the need to get close to objects of high temperature or in areas with limited accessibility due to safety restrictions. Second, it enables measurements of a large area simultaneously. However, this inherently brings one main disadvantage, the difficulty to locate the exact position of each pixel measured in the real environment. To overcome this issue we suggest the use of Augmented Reality (AR).

The term Augmented Reality refers to enhancing a user's view of the environment with additional computer-generated graphical information. Those virtual additions need to be seamlessly integrated into the environment, that is appear at the right location and with the right orientation, and be updated in real-time in order for the enhancement to be perceived as realistic. Different methods exist to achieve this augmentation: graphics are rendered into video streams on stationary monitors or hand-held devices like smartphones and tablets, or are presented on a head-mounted display integrated into a helmet. While these approaches allow for a realistic three-dimensional enhancement, they also limit the user's view to the screen of the augmented device, or require him to carry/wear the display hardware which may be cumbersome and might hinder him from performing his intended work. Furthermore, the enhancement is limited to those carrying the device.

Spatial Augmented Reality (SAR) [4] takes a different approach to realize those visualizations: projectors are employed to show the augmentation data directly in the user's surroundings. The user is freed from carrying any additional hardware and sees the data directly where he needs it: on the objects in his work environment. There is no need to (mentally) transfer the information from a visualization device to the real environment. While this approach limits augmentations to the setup area of the projector, multiple projectors can be used to increase the working range, or a portable projection system can be used, to change the display area to the need by hand.

In this paper we propose a system that combines thermal imaging with AR similar to the one recently presented by Palmerius and Schönborn[5]. By co-calibrating a thermal camera with a projector the visual representation of the temperature information is directly reprojected into the scene. This enables the user to perform visual inspection on manufacturing processes, to examine the run of electric systems or pipelines and to localize thermal leaks in buildings more easily. To account for errors due to the different perspective of the thermal camera and the projector a 3D camera is integrated as an additional component. The system is modular, as the components are interchangeable, and portable, as each indivdual component is mounted on a tripod. With only a few steps the system can be set up in any location. Compared to [5] it is easier to set up

978-1-5090-3549-6/16/$31.00

and covers a larger area, i.e., several meters. By using a pico projector it is technically possible to create a mobile system that works similar to a flashlight. However, current handheld projectors are limited in luminance and tracking is limited in accuracy, restricting the application areas of such a system. The paper describes the general workflow and the necessary steps to set up a system for spatial projection of thermal data for visual inspection. The approach is evaluated based on a small test scenario.

II. State of the Art

A. 3D Thermal modelling

The method of measuring temperatures through thermal imaging has one inherent disadvantage. It is often difficult to relate the heat information seen in the image precisely to its exact location in the environment. In typical applications for temperature analysis of buildings the data is recorded on the spot and the analysis is performed afterwards. This requires exact documentation of each image location and increases the recording time drastically. To overcome this issue recently methods have been proposed to create full 3D thermal models of buildings to facilitate the analysis of the recorded data. Different approaches have been used. The common idea is to co-calibrate a thermal camera with a sensor that allows the generation of 3D models. Ham and Golparvar-Fard [6] use structure from motion (SFM) on the images of an RGB camera to create the 3D model. SFM is prone to errors in regions with repeating structures or scarce features. The model generation is fully automatic but time consuming, leading to a low density model with unknown scale. The scale factor is overcome by using a 3D laser scanner [7], [8] as the resulting model has high geometric accuracy. The main drawbacks in this case are the high prices for 3D laser scanners and the long acquisition time for the 3D data. Depending on the desired resolution, acquiring a 3D laser scan takes from several seconds up to minutes. In the fastest operation mode the Riegl VZ-400 laser scanner operates with a resolution of 0.5° both horizontally and vertically requiring 6 s per scan. The Faro Focus operates at rates up to 1 Hz using the automation adapter. However, the data is not accessible in real time but needs to be extracted afterwards. In dynamic environments the low acquisition rates cause problems. Vidas et al. [9], [10] developed a hand-held system using an RGB-D camera. RGB-D cameras such as the Microsoft Kinect yield up to 30 frames per second which makes them suitable for real time applications. The main limitation is the accuracy of the resulting 3D data but the benefits of the fast acquisition time prevail for AR applications.

B. Spatial Augmented Reality

Spatial Augmented Reality has been employed in a number of different application areas, ranging from prototyping [11] and design [12], museum installations [13], maintenance, medical imaging, training, to operation and control of CNC machines [14] or manipulator robots [15]. To confine this overview, we limit ourselves to systems in combination with a depth camera, and some used for inspection. A system that combines projection based graphics with 3D-sensors is the RoomProjector/SLAMProjector by Molyneaux et al. [16]. Similar to our system, they use depth cameras to aquire depth data of the projection surface. Their projection system is handheld, i.e., it can be moved while using it. The movement of the projector is tracked with either multiple stationary depth cameras or a depth camera fixed to the projector, respectively. While offering great flexibility in choosing the augmented area, tracking accuracy of the handheld projector is limited in the first case, and prone to suffer from drift in certain cases in the second. This limits the achievable accuracy of the projected data, making this type of portability not ideal for our visual inspection purposes. The Beamatron system by Wilson et al. [17] combines a depth sensor with a projector mounted on a pan-tilt platform. While this steerable display setup is more complicated from a hardware point of view, it allows shifting the projection area and even tracking a moving user with high accuracy. Wilson uses the depth data for rendering of perspectively correct 3D-objects (requiring constant tracking of the user's position) as well as an environmental physics model, and allows speech and gesture guided interaction with the environment. An SAR system used for quality inspection of spot welding points in automotive manufacturing was presented by Zhou et al. [18]. The system allows to easily locate welding spots on the real car body by highlighting them with several SAR visualization options, avoiding the necessity to locate them on a technical drawing or monitor and to transfer that knowledge to find the corresponding spots in the work surroundings. Olwal et al. [14] use SAR in combination with a see-through glass panel with CNC-machinery. Real-time process data or occluded tools are made visible to the operator, allowing inspection and a better understanding of the process, and simplifying operation of the mill. Leutert et al. [15] use a SAR-system to display data in the workcell of an industrial manipulator. The processing path and the logged data are visualized directly on the workpiece, making the expected processing result visible before execution and allowing for easy inspection and modification with relation to the real work environment.

III. Methodology

A. System overview

The system for spatial projection of thermal data for visual inspection consists of three main hardware components. A thermal camera perceives the infrared radiation emitted from observed objects that corresponds to their temperature. A depth camera records the 3D geometry of the scene while the projector projects the observed information back into the scene to make the temperature values visible to the user. Each component defines its own coordinate system. The essential point is to determine the transformation between these coordinate systems and to transform the data accordingly. Fig. 1 shows the data flow in the system. The system is designed to be portable. Thermal camera, depth camera and projector are each individually mountable on tripods. Alternatively they can be fixed in a working environment. After each setup a one time

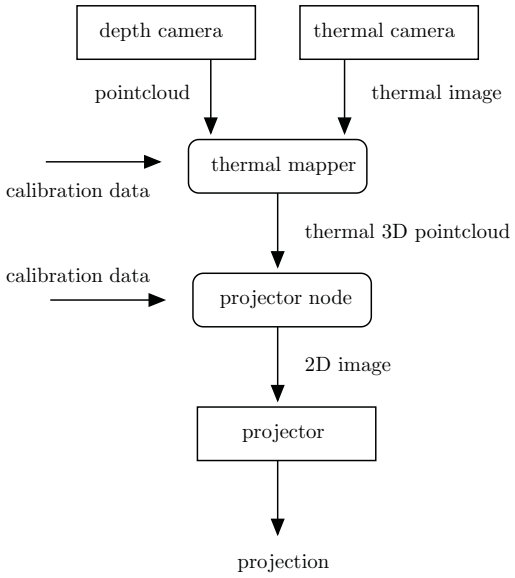

Fig. 1. Data flow diagram of the system.

calibration is necessary to calculate the new coordinate system transformations. Afterwards the system runs continously. The central link is the thermal 3D point cloud. It is linked to the global coordinate system. For ease of implementation in our test scenario the global coordinate system is identical to the coordinate system of the depth camera. However, integrating a given global coordinate system of the working environment requires only one further transformation. The depth camera acquires point clouds and the thermal camera acquires thermal images. These are combined into the thermal 3D pointcloud by the thermal mapper node. The projector node uses the calibration data for the projector to transform the point cloud into a 2D image that is projected into the scene. The following describes first the different calibration processes and then the workflow during runtime.

B. Calibration

Combining the individual hardware components of the system requires knowledge of their geometric properties. This is achieved by geometric calibration. The calibration consists of two parts, namely intrinsic and extrinsic calibration.

Intrinsic calibration for a camera describes the process of determining the internal parameters of the camera that define how a point in world coordinates is transformed into image coordinates, i.e. projected onto the image plane. The standard camera model consist of two parameters for the focal length, two coordinates for the camera center, three radial distortion coefficients and two tangential distortion coefficients. The standard method to determine them is to take images of a pattern with known features. The image coordinates of the features and their known relation in world coordinates are used to formulate a non-linear least squares problem that is solved using the Levenberg-Marquardt algorithm [19].

Extrinsic calibration refers to the process of determining the relative pose (orientation and translation) between two components. The prerequisite for extrinsic calibration is the intrinsic calibration of the devices.

The system for spatial projection of thermal data consists of three hardware components. Their calibration is described in this section. The thermal camera and the projector need to be intrinsically calibrated. As depth cameras are designed to measure geometric properties they are already geometrically calibrated. For the extrinsic calibration both the projector and the thermal camera are calibrated to the depth camera.

1) Intrinsic calibration of thermal camera: For the calibration of thermal cameras the calibration pattern has to be actively or passively heated for features to show up in the images [20]. Actively heated patterns are robustly detectable and do not require any special environment conditions. This is ideal for a portable system. Therefore the intrinsic calibration of the thermal camera in our approach is performed using a board with a uniform pattern of 5×6 small lightbulbs that are clearly distinguishable in the thermal image. With these features the approach for the intrinsic calibration of optical cameras is performed.

2) Intrinsic calibration of projector: As is fairly common in SAR systems, the projector in our system is modeled as an (inverse) pinhole camera. This allows for applying the same well-researched algorithms for calibration and image formation as are used in camera systems.

The input required for determining the internal and external calibration parameters of the device is a number of 2D/3D point pairs. In case of the projector this specifies where the light ray of an illuminated 2D pixel hits the corresponding 3D point in the environment. Since the internal parameters of a projector need to be determined only once, a more elaborate but precise method for calibration was chosen here. The point pairs were aquired by fixing and measuring an electronic board with light sensitive photo resistive elements on a precise positioning device, an industrial robot with absolute positioning error $< 0.1\,\mathrm{mm}$. The light sensor was moved to different positions in the projection volume of the projector, and the corresponding 2D pixel illuminating the photo resistor at that position was determined using binary search in the projector image.

This method of point pair determination requires specialized hardware. If not available, other, more easily realizable approaches to calibrate the projector might also be used, for example using a pre-calibrated camera [21].

3) Extrinsic calibration between thermal camera and depth camera: For calibration between the RGB-D camera (or any depth camera) and the thermal camera the same pattern is used as for the intrinsic calibration of the thermal camera, following the approach from [22], where a thermal camera is calibrated to a 3D laser scanner. Similar to a laser scanner the RGB-D camera produces a 3D point cloud. As the lightbulbs are uniformly positioned on a board, their position is derived from the position of the board. To detect the board the RANSAC algorithm is used that finds the most prominent plane in the point cloud. A model of the board is then transformed into the

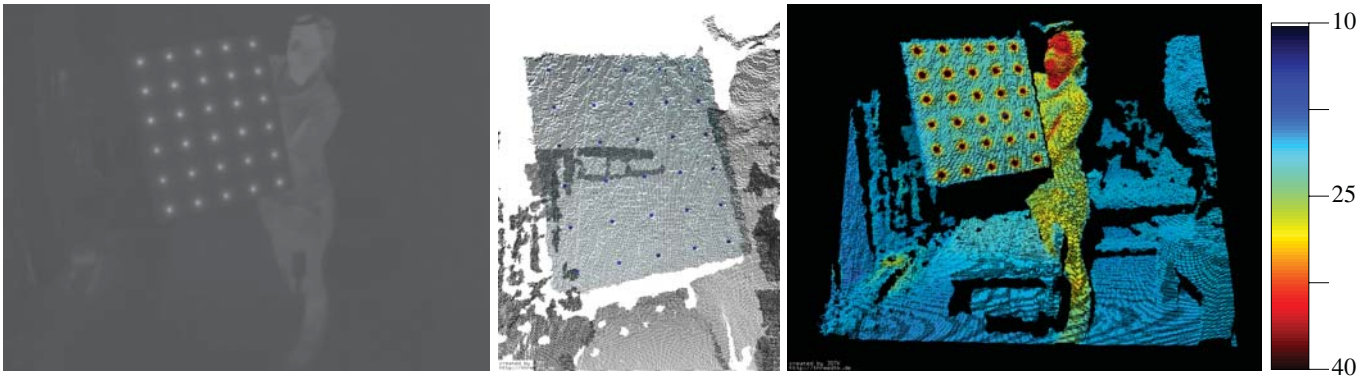

Fig. 2. The generation of the thermal point cloud. (a) Thermal image in grayscale (white $\hat{=}$ 0°, black $\hat{=}$ 100°). (b) The calibration procedure. The model (cyan) is fitted to the data to determine the position of the light bulbs (blue). (c) The points are colored based on the scale shown in (d).

center of the detected plane and the ICP algorithm (iterative closest point [23]) is used to fit the model into the data points, yielding the position of the board and the position of the lightbulbs simultaneously. From the thus calculated correspondences and the known intrinsic calibration of the thermal camera the rotation and translation is calculated. This procedure is applied repeatedly to minimize the error. To automate the calibration a bounding box is placed around all patterns and all points outside of the bounding box are removed. The resulting transformation is validated by verifying that each point from the model is within a threshold of one data point. The calibration process in illustrated in Fig. 2. Fig. 2(a) shows a thermal image of the calibration pattern and Fig. 2(b) the corresponding point cloud, respectively. The model of the calibration pattern is depicted in cyan. It is aligned to the data so that the blue points mark the position of the lightbulbs in the point cloud. Based on the feature pairs in the thermal image and the point cloud the transformation between the two sensors is calculated.

4) Extrinsic calibration between projector and RGB-D camera: Several different approaches already exist to calibrate the extrinsic parameters between a camera and projector pair. Those involve, for example, using a pre-calibrated camera to find correspondences for camera and projector in world coordinates of some calibration object. Other approach are to adjust a projected pattern iteratively until it matches a printed one, or to find a homography transformation between a calibration plane and the projector image plane.

For our system we use the approach proposed in [24], where corners of a chessboard pattern are detected in the camera and projector image, and local homographies for each detected corner are computed. Using a printed chessboard pattern increases complexity of the calibration procedure slightly, but allows to account for non-linearities in the optics of the projector and results in high accuracy calibration data.

During this procedure, images from the RGB-D-camera are used to determine chessboard corners and to capture structured light illumination from the projector. This allows to detect the pixel location of those corners with subpixel accuracy from the camera as well as from the projector, resulting in high quality input for the calibration algorithm that computes the transformation data between projector and RGB-D camera.

C. Thermal projection pipeline

After calculating the calibration parameters the projection pipeline as depicted in in Fig. 1 is straightforward. Given the calibration of the thermal camera with respect to the RGB-D camera the point cloud is projected onto the image plane to determine for each point the corresponding temperature value. The point cloud is then transferred to the projector node where each point is transformed into the projector coordinate system. To create a 2D image each point is projected onto the projector plane. On each pixel a z-buffer is applied that removes all points except the closest point accounting for occlusions in the environment from the perspective of the projector. For those pixels containing a point the color is calculated from the temperature value. Humans typically associate colors in the red spectrum to warm temperatures and colors in the blue spectrum to cold temperatures. Based on this association an adjustable color scale is developed, as depicted in Fig. 2(d). For the point cloud seen in Fig. 2(c) the temperature limits are set to $10^\circ\,\mathrm{C} \ldots 40^\circ\,\mathrm{C}$. Pixels without a point remain blank. The resulting image is sent to the projector output. This procedure is repeated in real time to show dynamic changes in the environment continuously.

D. Combination with a tracked input device

In order to not only see the temperature data visualized in the environment, but also take precise measurements at specific spots of interest in the work area (as with a probe) the operator needs to be able to specify the 3D-coordinates of the desired measurement spot. For this purpose, different tracking systems and input devices could be used, ranging from simple tracking of gestures up to using commercially available high-precision tracking systems. In the system presented here we used the already available pen tracking system from [15]. For RGB-D cameras skeleton tracking is already available. Another possibility would be to build upon this by using the operators

Fig. 3. Hardware used in the experiments, a Panasonic PT-VZ575N projector, an Asus Xtion Pro live RGB-D camera and an optris PI 400 thermal camera.

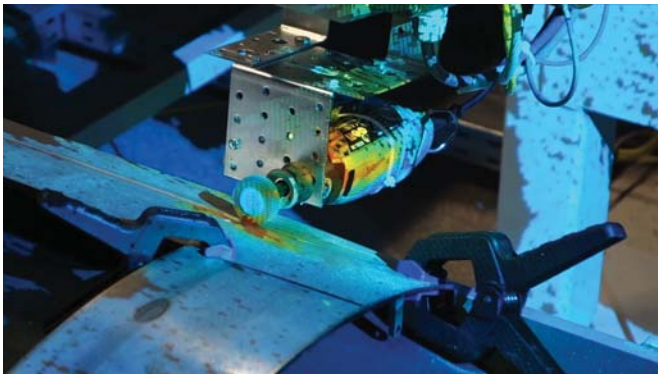

Fig. 4. Display of temperatures during processing: the heat developing on the surface due to the grinding, as well as in the motor of the tool becomes clearly visible.

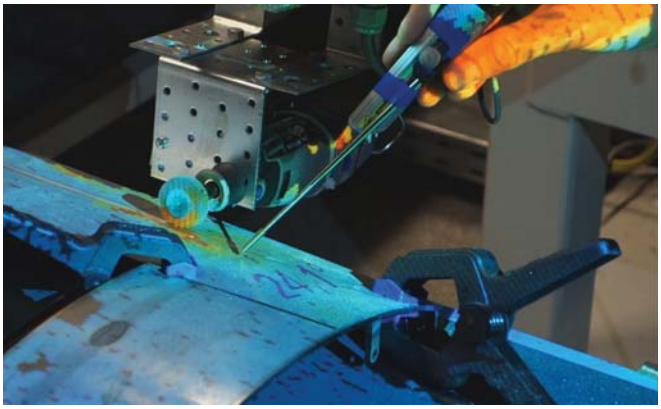

Fig. 5. Measurement of surface temperature of the metal workpiece shortly after processing, using a tracked probe to specify the measurement point.

hands as system input. This option comes with no additional hardware but is limited in terms of accuracy. The specified probe coordinates must then be transformed to the coordinate system of the point cloud which is easily possible, since all involved systems have been calibrated beforehand.

For the global probe coordinates, the closest point in the aquired point cloud of the environment is determined. If point data is available and sufficiently close to the coordinates indicated by the user, the precise temperature and spot the data is taken from is marked and displayed in the projection image. By highlighting the measurement spot again the user can be certain of where precisely a temperature reading is taken from, which might be important if a less precise tracking system were to be used. This allows the user to not only see the general heat distribution in the environment, but also take precise numerical readings at certain critical spots, and enhances the functionality of the system significantly.

IV. Experiments and Results

A. Setup

The proposed approach is evaluated using a small test case. The hardware for 3D measurements in the scenario is an Asus Xtion Pro Live RGB-D camera. It operates best at a distance of 0.8 to 3.5 m at an opening angle of $58° \times 45°$. The depth image has a resolution of 640×480 pixels, the RGB image a resolution of 1280×1024 pixels with 30 frames per second. The thermal camera used in the scenario is an optris PI400. With a field of view of $62° \times 49°$ at $f = 8\,\mathrm{mm}$ it has an optical resolution of 382×288 pixels at a frame rate of up to 80 Hz. In the temperature range from $-20°\,\mathrm{C}$ to $100°\,\mathrm{C}$ it features a thermal sensitivity of $0.8\,\mathrm{K}$. The Panasonic PT-VZ575N is a portable projector capable of a resolution of 1920×1200 pixels at 4,800 lm. The hardware (depicted in Fig. 3) is set up in the work cell of a KUKA KR 16 industrial robot.

B. Evaluation

For a first evaluation, a small processing task was set up. The industrial robot was programmed to polish a metal workpiece. This workpiece, a metal oven door, was fixed in the work cell. For the actual processing, a small grinding tool was mounted onto the manipulator, and a simple processing path specified for the robot. The heat inspection system was set up and calibrated to capture the work execution.

During the evaluation runs, the developing heat when the tool was in contact with the workpiece, grinding the metal surface, was clearly made visible as seen in Fig. 4. Due to a relative high amount of pressure during processing, a lot of strain was put on the electromagnetic motor of the small processing tool, resulting also in a high internal temperature, which could also readily be seen in the reprojection. Precise temperature readings were taken using a tracked probe system as described earlier. The increase in temperature at the grinding spot, although small due to the limited size and power of the employed processing, and subsequent cooling down of the metal could visualized and measured numerically (cf. Fig.5).

In a second experiment the spatial accuracy of the reprojection system is tested and visualized. The wooden calibration pattern featuring small light bulbs in a regular distance grid was placed in front of the system. Since the wood stays relatively cool compared to the light bulbs, the measured heat distribution around the light centers, and thus the spatial accuracy of the thermal inspection system could be visually verified as exemplarily shown in Fig. 6.

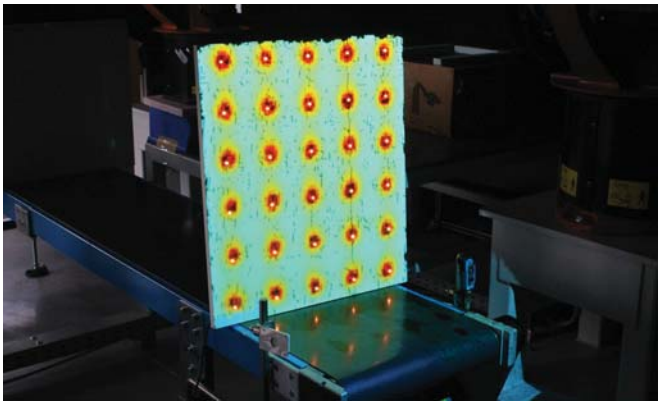

Fig. 6. The thermal reprojection of the temperature distribution of the calibration pattern for the thermal camera. It becomes clearly that the area around the small light bulbs is heated up.

From 32 frames of a video recording featuring the board at different positions between 164 cm and 281 cm from the depth camera, the light bulbs and their projection were manually selected. After applying a a perspective transform to descew the pattern an average reprojection error of 11.198 mm was computed. Analyzing the results revealed a small systematic error. As the default calibration between the depth and the color image from the RGB-D camera was used in this experiment the overall spatial accuracy is expected to increase when applying a custom refinement of the calibration.

The experiments showed that the system is capable of projecting the thermal information into the seen facilitating visual inspection. In both experiments the system had to deal with dynamic changes in the environment. An average framerate of approximately 13 Hz was suitable to visualize these changes in realtime. More systematic and precise numerical evaluations of the spatial reprojection accuracy as well as temperature measurement accuracy are currently underway.

V. Conclusion

We presented a portable system for visual inspection of temperature related changes in the environment. In the first proof of concept it visualizes the thermal information in dynamic environments in realtime. For its practical applicability further improvements are necessary. To enhance the visual information we plan to apply color correction to compensate for the color in the environment. The accuracy of the temperature measurements relies on the quality of the thermal camera. However, the various calibration steps influence the spatial accuracy of the system. Further systematic and numerical evaluations of the projection accuracy of the system are necessary. This includes the evaluation of the individual components as well as their impact on the accuracy of the entire system.

References

[1] N. A. Fouad and T. Richter, *Leitfaden Thermografie im Bauwesen – Theorie, Anwendungsgebiete, praktische Umsetzung*, 4th ed. Stuttgart: Fraunhofer IRB Verlag, 2012.

[2] Optris GmbH, *Optris Infrared Thermometers: Applications*, http://www.optris.com/automotive.

[3] Jacob Plastics Group, "Application Story: Shortage production considerably reduced with thermal imager optris PI," http://www.optris.com/temperature-measurement-automotive, Optris GmbH, Tech. Rep., accessed on 27.04.2016.

[4] O. Bimber and R. Raskar, *Spatial augmented reality: merging real and virtual worlds*. CRC Press, 2005.

[5] K. L. Palmerius and K. Schönborn, "Visualization of heat transfer using projector-based spatial augmented reality," in *Int. Conf. Augmented Reality, Virtual Reality, Comp. Graphics*. Springer, 2016, pp. 407–417.

[6] Y. Ham and M. Golparvar-Fard, "An automated vision-based method for rapid 3D energy performance modeling of existing buildings using thermal and digital imagery," *Advanced Engineering Informatics*, 2013.

[7] Borrmann, D. and Nüchter, A. and Đakulović, M. and Maurović, I. and Petrović, I. and Osmanković, D. and Velagić, J., "A mobile robot based system for fully automated thermal 3D mapping," *Advanced Engineering Informatics*, vol. 28, no. 4, pp. 425–440, October 2014.

[8] D. González-Aguilera, P. Rodriguez-Gonzalvez, J. Armesto, S. Lagüela, "Novel approach to 3D thermography and energy efficiency evaluation," *Energy and Buildings*, vol. 54, pp. 436–443, 2012.

[9] S. Vidas, P. Moghadam, and M. Bosse, "3D Thermal Mapping of Building Interiors Using an RGB-D and Thermal Camera," in *Proc. of the IEEE Conf. on Robotics and Automation (ICRA '13)*, May 2013.

[10] Stephen Vidas, Peyman Moghadam, "HeatWave: A handheld 3D thermography system for energy auditing," *Energy and Buildings*, vol. 66, pp. 445–460, November 2013.

[11] S. R. Porter, M. R. Marner, R. T. Smith, J. E. Zucco, and B. H. Thomas, "Validating spatial augmented reality for interactive rapid prototyping," in *Mixed and Augmented Reality (ISMAR), 2010 9th IEEE International Symposium on*. IEEE, 2010, pp. 265–266.

[12] M. R. Marner and B. H. Thomas, "Augmented foam sculpting for capturing 3d models," in *3D User Interfaces (3DUI), 2010 IEEE Symposium on*. IEEE, 2010, pp. 63–70.

[13] B. Ridel, P. Reuter, J. Laviole, N. Mellado, N. Couture, and X. Granier, "The revealing flashlight: Interactive spatial augmented reality for detail exploration of cultural heritage artifacts," *Journal on Computing and Cultural Heritage (JOCCH)*, vol. 7, no. 2, p. 6, 2014.

[14] A. Olwal, J. Gustafsson, and C. Lindfors, "Spatial augmented reality on industrial CNC-machines," in *Electronic Imaging 2008*. International Society for Optics and Photonics, 2008, pp. 680 409–680 409.

[15] F. Leutert, C. Herrmann, and K. Schilling, "A spatial augmented reality system for intuitive display of robotic data," in *Proceedings of the 8th ACM/IEEE international conference on Human-robot interaction*. IEEE Press, 2013, pp. 179–180.

[16] D. Molyneaux, S. Izadi, D. Kim, O. Hilliges, S. Hodges, X. Cao, A. Butler, and H. Gellersen, "Interactive environment-aware handheld projectors for pervasive computing spaces," in *Pervasive Computing*. Springer, 2012, pp. 197–215.

[17] A. Wilson, H. Benko, S. Izadi, and O. Hilliges, "Steerable augmented reality with the beamatron," in *Proceedings of the 25th annual ACM symposium on User interface software and technology*. ACM, 2012, pp. 413–422.

[18] J. Zhou, I. Lee, B. Thomas, R. Menassa, A. Farrant, and A. Sansome, "In-situ support for automotive manufacturing using spatial augmented reality," *The International Journal of Virtual Reality*, vol. 11, no. 1, pp. 33–41, 2012.

[19] Z. Zhang, "Flexible camera calibration by viewing a plane from unknown orientations," in *in ICCV*, 1999, pp. 666–673.

[20] T. Luhmann, J. Piechel, J. Ohm, and T. Roelfs, "Geometric calibration of thermographic cameras," in *International Archives of Photogrammetry, Remote Sensing and Spatial Information*, vol. 38 part 5, Newcastle upon Tyne, UK, 2010, Commission V Symposium.

[21] M. Kimura, M. Mochimaru, and T. Kanade, "Projector calibration using arbitrary planes and calibrated camera," in *Proc. IEEE Conf. on Computer Vision and Pattern Recognition (CVPR)*. , 2007, pp. 1–2.

[22] D. Borrmann, H. Afzal, J. Elseberg, and A. Nüchter, "Mutual Calibration for 3D Thermal Mapping," in *Proceedings of the 10th Symposium on Robot Control (SYROCO)* , Dubrovnik, Croatia, September 2012.

[23] P. J. Besl and N. D. McKay, "A Method for Registration of 3-D Shapes," *IEEE Transactions on Pattern Analysis and Machine Intelligence*, vol. 14, no. 2, pp. 239 – 256, February 1992.

[24] D. Moreno and G. Taubin, "Simple, accurate, and robust projector-camera calibration," in *2nd International Conference on 3D Imaging, Modeling, Processing, Visualization and Transmission (3DIMPVT)*. IEEE, 2012, pp. 464–471.